Supplemental Data

Uromodulin p.Cys147Trp mutation causes kidney disease by ER-stress/TNF-mediated apoptosis

Bryce G. Johnson[1,2], Lan T. Dang[1], Graham Marsh[1], Allie M. Roach[1,2], Zebulon G. Levine[1], Anthony Monti[1], Deepak Reyon[1], Lionel Feigenbaum[1]* & Jeremy S. Duffield[1,2,3] *

1. Supplemental Figures:

Figure S1

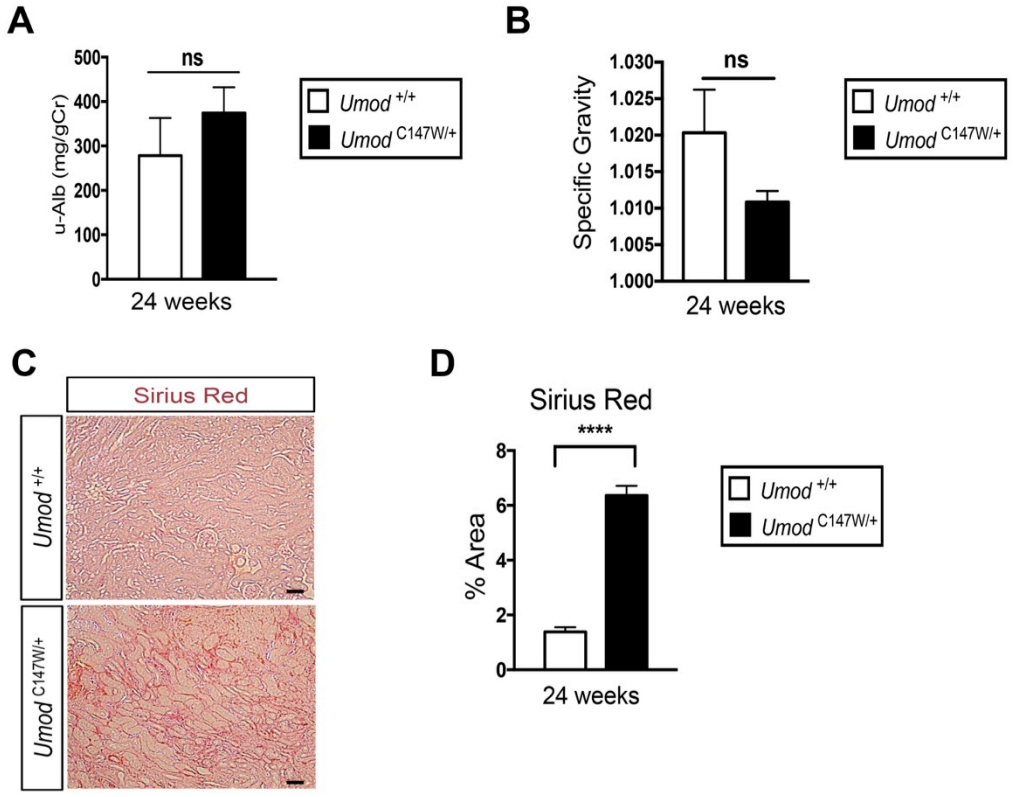

Figure S1. *Umod* $^{C147W/+}$ mice exhibit mild proteinuria and severe tissue fibrosis.
(A) Urinary albumin (u-Alb) quantified from 24-week-old mice. (B) Specific gravity measured in urine of 24-week-old mice. (C) Histological images of whole kidney sections (4µm) stained with Picrosirius red preparation (collagens I/III in red). Images taken at 10X. (D) Quantification of Picrosirius Red images. Data are represented as mean ± SEM. *P<0.05, **P<0.01, ***P<0.001, ****P<.0001. Student's t-test. n = 6–8 per group. (Scale bars, 50 μ m.)

Figure S2

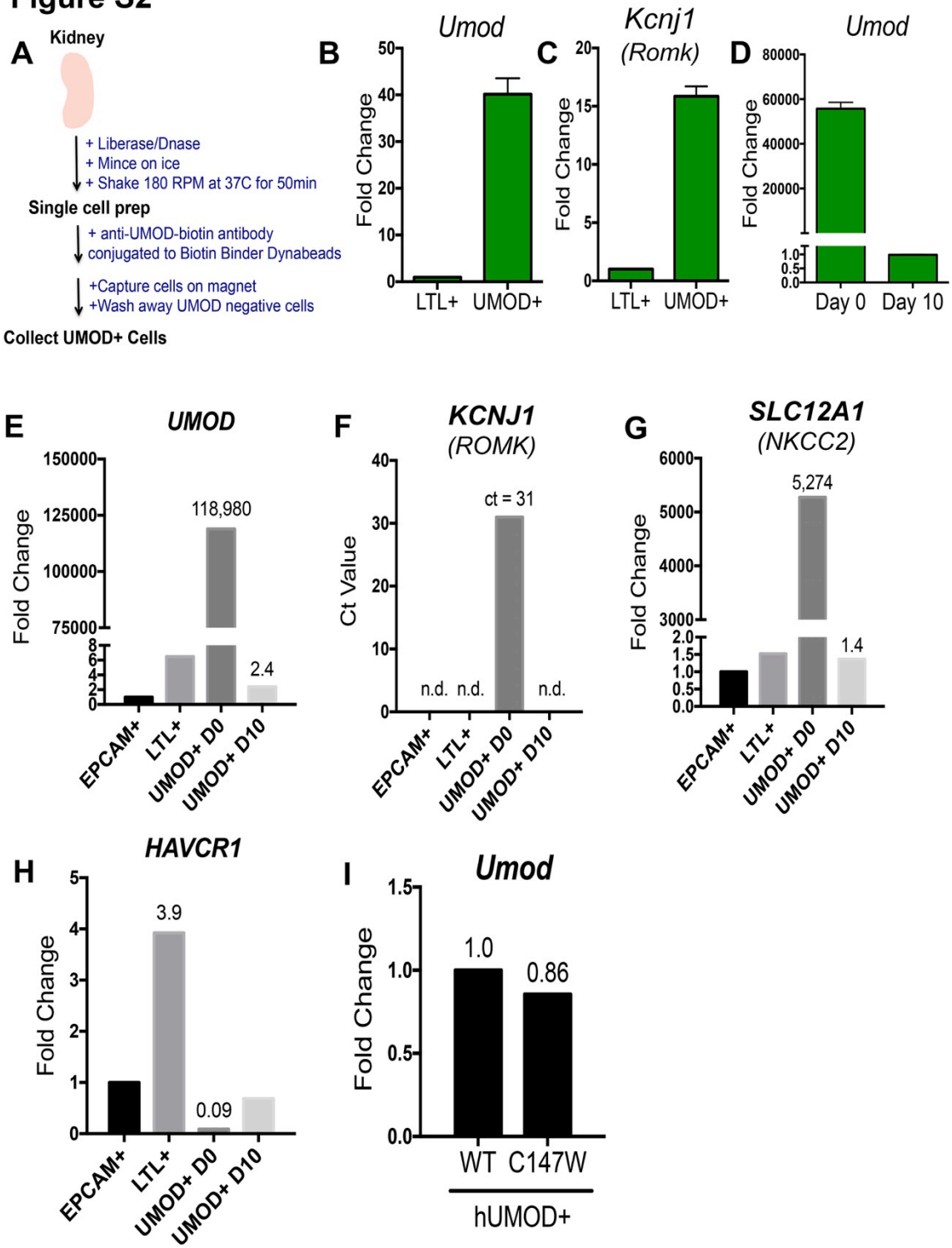
A
Kidney
+ Liberase/Dnase
+ Mince on ice
+ Shake 180 RPM at 37C for 50min
Single cell prep
+ anti-UMOD-biotin antibody
conjugated to Biotin Binder Dynabeads
+Capture cells on magnet
+Wash away UMOD negative cells
Collect UMOD+ Cells
B
Umod
Fold Change
LTL+
UMOD+
C
Kcnj1
(Romk)
Fold Change
LTL+
UMOD+
D
Umod
Fold Change
Day 0
Day 10
E
UMOD
Fold Change
118,980
2.4
EPCAM+
LTL+
UMOD+ D0
UMOD+ D10
F
KCNJ1
(ROMK)
Ct Value
ct = 31
n.d.
n.d.
n.d.
EPCAM+
LTL+
UMOD+ D0
UMOD+ D10
G
SLC12A1
(NKCC2)
Fold Change
5,274
1.4
EPCAM+
LTL+
UMOD+ D0
UMOD+ D10
H
HAVCR1
Fold Change
3.9
0.09
EPCAM+
LTL+
UMOD+ D0
UMOD+ D10
I
Umod
Fold Change
1.0
0.86
WT
C147W
hUMOD+

Figure S2. Isolation of primary Uromodulin producing epithelial cells.

(A) Schema for UMOD producing cell isolation procedure using Biotin Binder Dynabeads. (B-C) Quantification by q-PCR of gene expression in Day 0 UMOD producing cell fraction and proximal LTL+ cell fraction from whole kidney isolate of 6-week-old Umod +/+ mouse. (B) *Umod* expression. (C) *Romk* expression. (D) Quantitative PCR of *Umod* expression in isolated, murine UMOD producing cells at Day 0 and Day10 post isolation from whole kidney. Note loss of *Umod* expression in Day 10 cells. (E-H) Quantification by q-PCR of gene expression in EPCAM+, LTL+, and UMOD producing Day 0 and Day 10 isolated cell fractions from human kidney isolate. Isolation of each cell type was performed sequentially from the same donor tissue, starting with UMOD, followed by EPCAM and then LTL. (E) *UMOD* expression. Note enrichment in UMOD producing Day 0 fraction, and drastic loss by Day 10. (F) *ROMK* expression reported as Ct value. Note no detection (n.d.) was observed after 40 cycles for EPCAM+, LTL+, and UMOD producing Day 10 isolates. (G) *NKCC2* expression. Note reduced expression in UMOD producing cells by Day 10. (H) *HAVCR1* (KIM1) expression. Note enrichment in proximal tubule LTL+ fraction. (I) Quantitative PCR of Uromodulin expression in human cell lines generated with lenti viral vectors harboring coding sequences for either the wild type or p.Cys147Trp mutant forms of Uromodulin. Note comparable expression levels. Representative data from 1 of 3 (B-D) or 1 of 4 (E-I) experiments are shown. n = 3-4 per group.

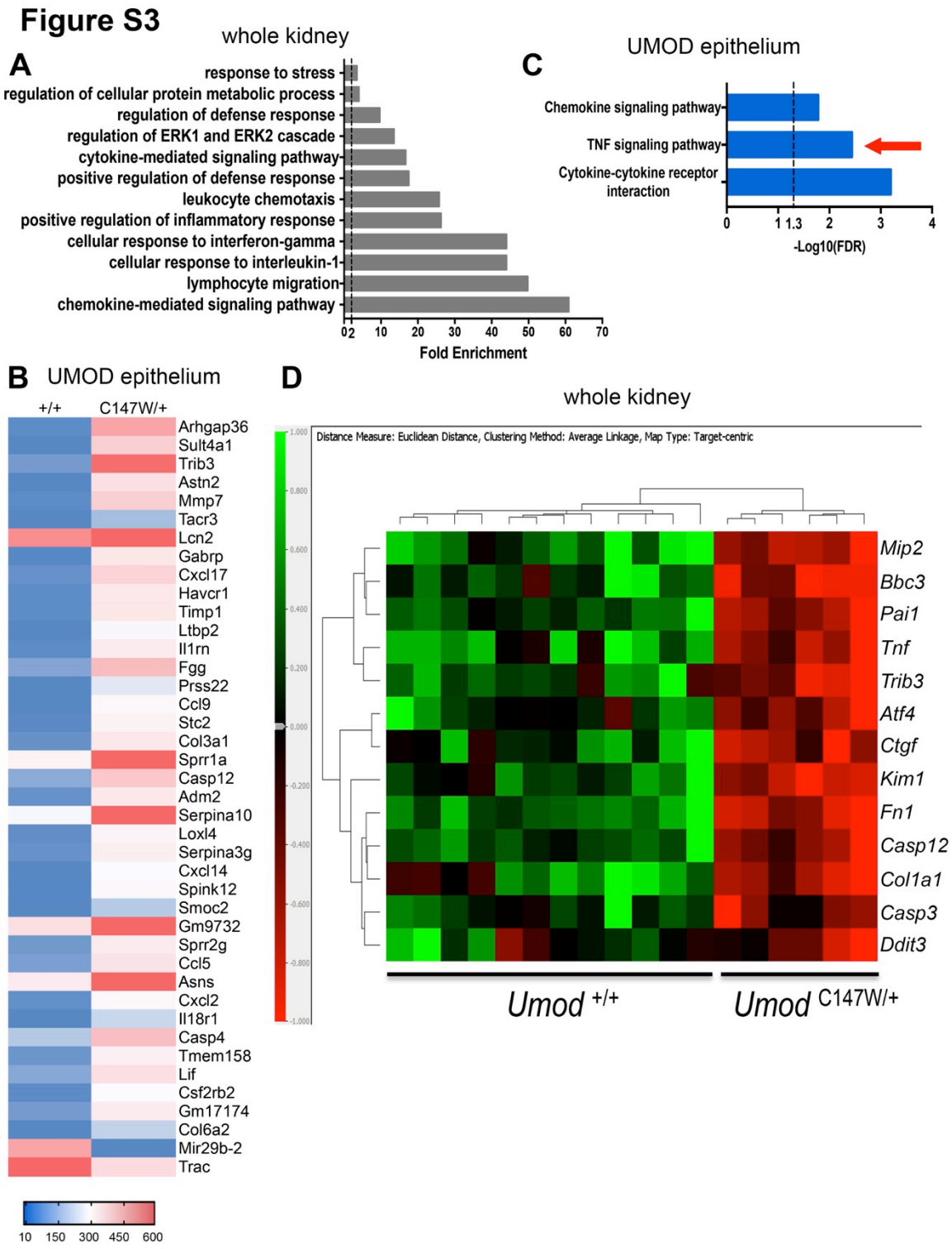
Figure S3
A
whole kidney
response to stress
regulation of cellular protein metabolic process
regulation of defense response
regulation of ERK1 and ERK2 cascade
cytokine-mediated signaling pathway
positive regulation of defense response
leukocyte chemotaxis
positive regulation of inflammatory response
cellular response to interferon-gamma
cellular response to interleukin-1
lymphocyte migration
chemokine-mediated signaling pathway
0 2 10 20 30 40 50 60 70
Fold Enrichment
C
UMOD epithelium
Chemokine signaling pathway
TNF signaling pathway
Cytokine-cytokine receptor interaction
0 1 1.3 2 3 4
-Log10(FDR)
B
UMOD epithelium
+/+
C147W/+
Arhgap36
Sult4a1
Trib3
Astn2
Mmp7
Tacr3
Lcn2
Gabrp
Cxcl17
Havcr1
Timp1
Ltbp2
Il1rn
Fgg
Prss22
Ccl9
Stc2
Col3a1
Sprr1a
Casp12
Adm2
Serpina10
Loxl4
Serpina3g
Cxcl14
Spink12
Smoc2
Gm9732
Sprr2g
Ccl5
Asns
Cxcl2
Il18r1
Casp4
Tmem158
Lif
Csf2rb2
Gm17174
Col6a2
Mir29b-2
Trac
10 150 300 450 600
D
whole kidney
Distance Measure: Euclidean Distance, Clustering Method: Average Linkage, Map Type: Target-centric
Mip2
Bbc3
Pai1
Tnf
Trib3
Atf4
Ctgf
Kim1
Fn1
Casp12
Col1a1
Casp3
Ddit3
Umod +/+
Umod C147W/+

Figure S3. Transcriptional Analysis of *Umod* $^{C147W/+}$ kidneys.

(A) GO results for biological process analysis from 40 most up-regulated DEGs from RNA from whole kidney isolate of 12-week-old mice kidneys (adjusted p-value <0.05; Fold enrichment >2). (B) Heat map of 40 most upregulated DEGs with adjusted p-value < 0.05 and $Log_2FC>1$. RNA isolated from UMOD producing cells from kidney tissue of 12-week –old mice. Scale bar in FPKM. (C) Enriched GO terms (adjusted p-value <0.05) from KEGG pathway analysis of the 40 most upregulated DEGs in RNA isolated from UMOD producing cells from kidney tissue of 12-week –old mice. (D) Heat map representation of q-PCR panel for key genes related to inflammation, fibrosis, apoptosis, UPR, and autophagy. Panel performed on 24-week-old whole kidney RNA isolate. Color-scale (red upregulated, green downregulated, black intermediate expression). n = 8-11 per group.

Figure S4

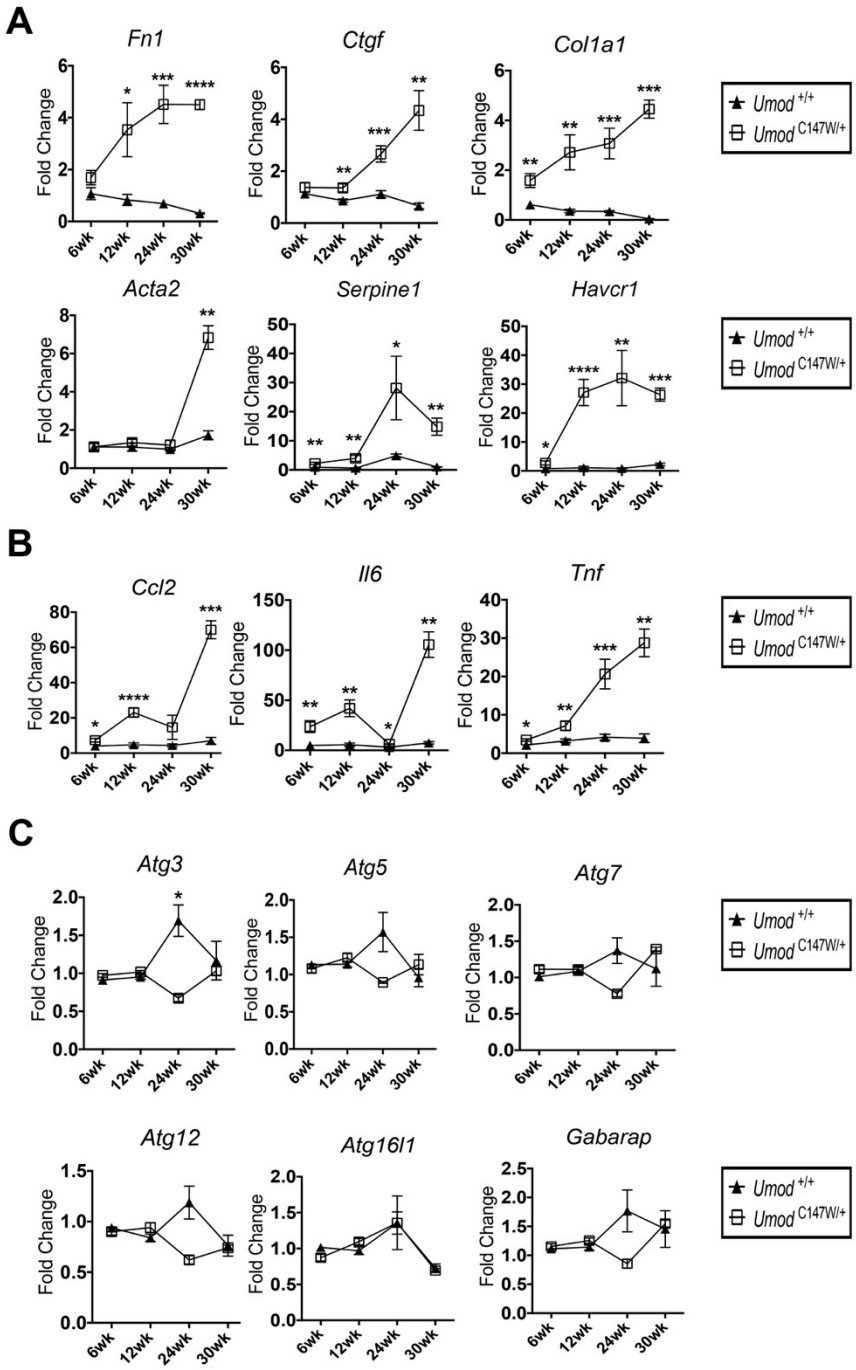
A
Fn1
Ctgf
Col1a1
Acta2
Serpine1
Havcr1
Fold Change
6wk
12wk
24wk
30wk
Umod +/+
Umod C147W/+
B
Ccl2
Il6
Tnf
C
Atg3
Atg5
Atg7
Atg12
Atg16l1
Gabarap

Figure S4. Time course analysis of transcriptional changes in *Umod* $^{C147W/+}$ kidneys.
(A-B) Quantitative PCR of RNA isolate from whole kidney tissue over time. (A) Fibrosis genes and Kidney Injury Molecule-1 (*Havcr1*). (B) Inflammatory genes. (C) Quantification of additional autophagy related genes by q-PCR from directly isolated UMOD producing primary murine epithelial cells over time. Data are represented as mean ± SEM. *P<0.05, **P<0.01, ***P<0.001, ****P<.0001. 2-way ANOVA with post hoc testing. n = 6–8 per group. (Scale bars, 50 μ m.)

Figure S5

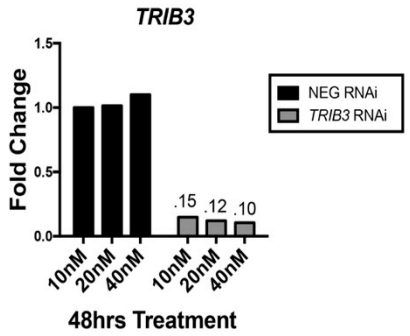

Figure S5. Tribbles-3 (*TRIB3*) silencing in human UMOD producing cells.
Quantification of expression of *TRIB3* 48hrs following treatment with siRNA; negative control or *TRIB3* (10-40nM). n= 2-3 per condition.

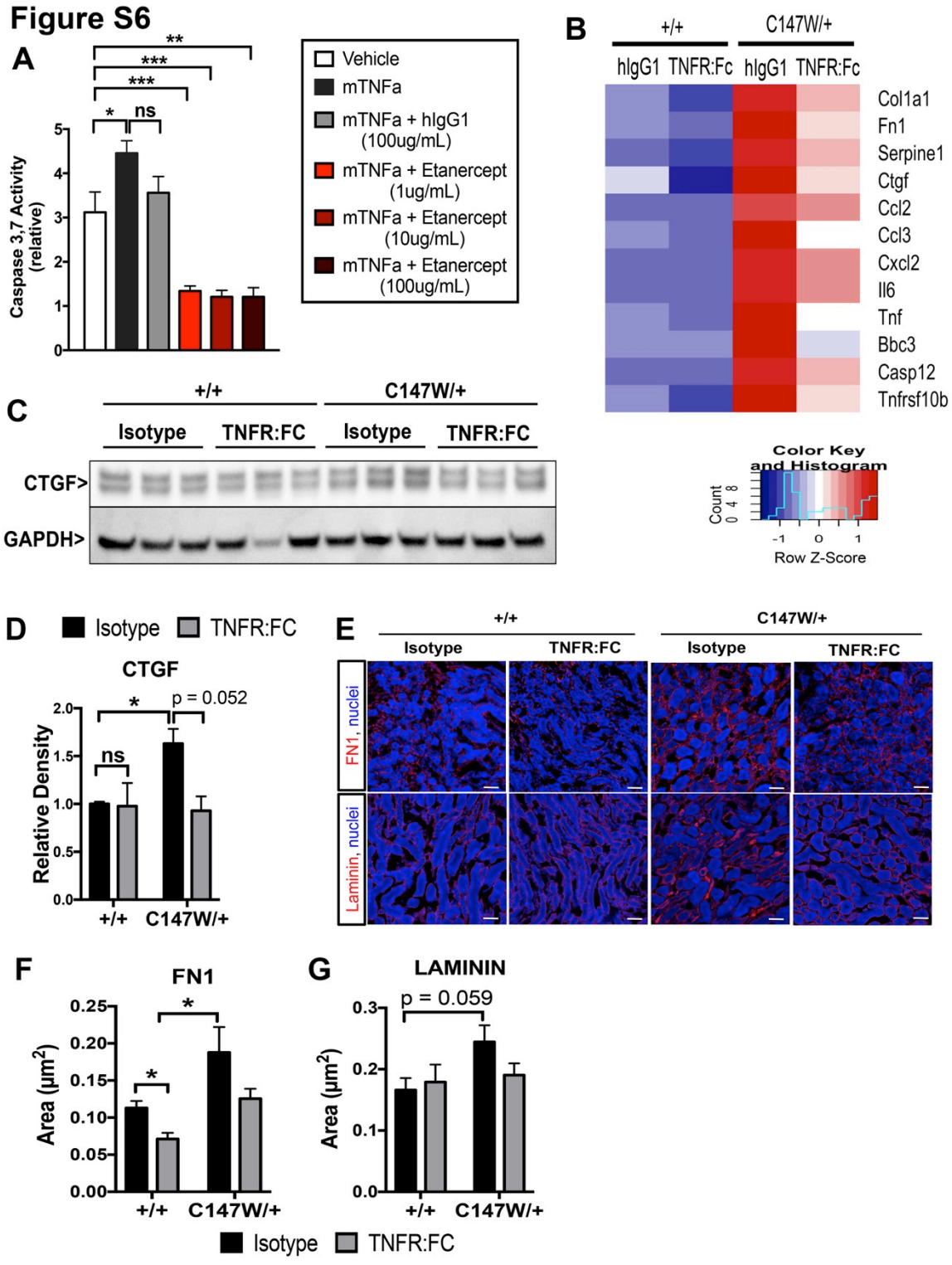
Figure S6
A
Caspase 3,7 Activity (relative)
Vehicle
mTNFa
mTNFa + hIgG1 (100ug/mL)
mTNFa + Etanercept (1ug/mL)
mTNFa + Etanercept (10ug/mL)
mTNFa + Etanercept (100ug/mL)
B
+/+
C147W/+
hIgG1 TNFR:Fc hIgG1 TNFR:Fc
Col1a1
Fn1
Serpine1
Ctgf
Ccl2
Ccl3
Cxcl2
Il6
Tnf
Bbc3
Casp12
Tnfrsf10b
Color Key and Histogram
Count
Row Z-Score
C
+/+
C147W/+
Isotype
TNFR:FC
Isotype
TNFR:FC
CTGF>
GAPDH>
D
Isotype
TNFR:FC
CTGF
Relative Density
p = 0.052
ns
+/+
C147W/+
E
+/+
C147W/+
Isotype
TNFR:FC
Isotype
TNFR:FC
FN1, nuclei
Laminin, nuclei
F
FN1
Area (µm2)
+/+
C147W/+
G
LAMININ
p = 0.059
Area (µm2)
+/+
C147W/+
Isotype
TNFR:FC

Figure S6. TNFR:Fc in vitro and in vivo experiments.

(A) Quantification of caspase-3,7 activity in human UMOD producing cells after 24hrs of treatment with vehicle, TNFα (50ng/mL) +/- hIgG control (100ug/mL) or TNFR:Fc 1, 10, 100μg/mL. n = 3 wells per condition. (B) Heat map of quantitated expression by q-PCR of fibrosis, inflammation, and apoptosis related genes. Scale reflects row Z-score of relative fold change normalized to wild type animals treated with isotype control antibody. (C) Western blot analysis of CTGF from whole kidney isolate of mice at 16 weeks-of-age +/- hIgG or TNFR:Fc. Note: blot from Figure 8B was stripped and re-probed for CTGF. (D) Densitometry of CTGF western blot. Note reduction of CTGF protein (p-value = 0.052) in heterozygous mice treated with TNFR:Fc. (E) Immuno-fluorescent images taken at 20X of fibronectin and laminin protein in whole kidney tissue sections. (F-G) Quantification of positively stained area (um^2). (F) Fibronectin area. (G) Laminin area. Data are represented as mean ± SEM. *P<0.05, **P<0.01, ***P<0.001, ****P<.0001. 2-way ANOVA with post hoc testing. n = 4-6 animals per group. (Scale bars, 50 μ m.)

Figure S7

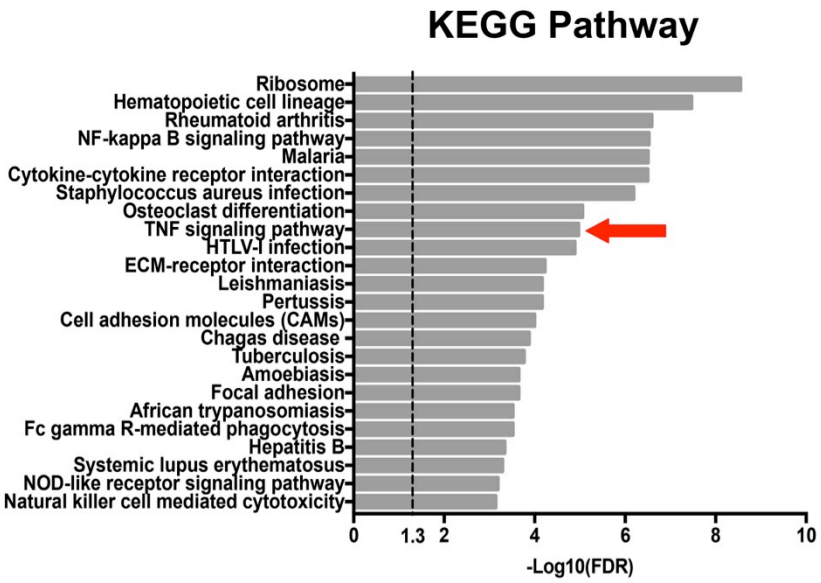

Figure S7. RNA sequencing of hypertensive and diabetic chronic kidney disease identifies TNF-signaling pathway enriched in upregulated genes compared to healthy matched controls.

GO results for KEGG pathway analysis from up-regulated DEGs from whole kidney isolate. (adjusted p-value <0.05; Fold enrichment >5). Note enrichment of TNF signaling pathway.

Figure S8

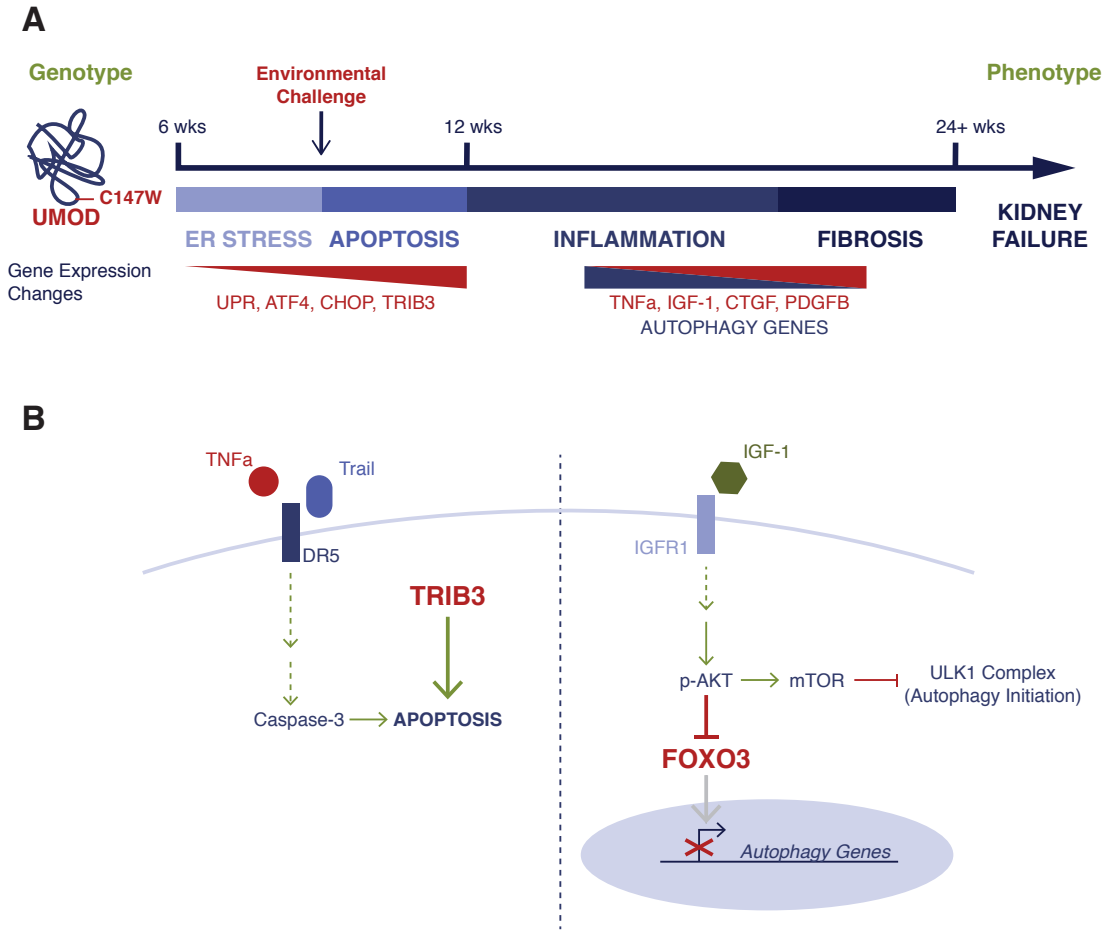
A
Genotype
Environmental Challenge
Phenotype
6 wks
12 wks
24+ wks
C147W
UMOD
ER STRESS
APOPTOSIS
INFLAMMATION
FIBROSIS
KIDNEY FAILURE
Gene Expression Changes
UPR, ATF4, CHOP, TRIB3
TNFa, IGF-1, CTGF, PDGFB
AUTOPHAGY GENES
B
TNFa
Trail
DR5
TRIB3
Caspase-3
APOPTOSIS
IGF-1
IGFR1
p-AKT
mTOR
ULK1 Complex
(Autophagy Initiation)
FOXO3
Autophagy Genes

Figure S8. Mechanism of disease progression.

(A) Timeline representation of disease progression from genotype to phenotype from 6wk to 24+ weeks. Mutant UMOD p.Cys147Trp protein triggers ER stress and UPR mechanisms, accumulating over time, which results in elevated ATF4, CHOP, TRIB3. Progressive fibrosis reaches peak at 24+weeks, concomitant with kidney failure. (B) Mechanistic representation for tubule apoptosis and autophagy inhibition. Trib3 acts as an intrinsic ER-stress mediated cell death mediator to sensitize UMOD producing tubular cells to TNF and TRAIL-induced apoptosis. Inhibition of autophagy is realized by elevated IGF-1, which positively regulates AKT. This in turn increases negative regulation of FOXO3, maintaining the transcription factor in the cytoplasm, preventing it from inducing expression of autophagy related genes. Active AKT positively regulates mTOR, which in turn inhibits the ULK1 complex, preventing phagophore formation and autophagy initiation.

2. Supplemental Tables:

Table S1

Gene	Taqman Probe	Species
Acta2	Mm00725412_s1	Mouse
Atf4	Mm00515325_g1	Mouse
Atg10	Mm00470550_m1	Mouse
Atg12	Mm00503201_m1	Mouse
Atg14	Mm00553733_m1	Mouse
Atg16l1	Mm00513085_m1	Mouse
Atg3	Mm00471287_m1	Mouse
Atg5	Mm00504340_m1	Mouse
Atg7	Mm00512209_m1	Mouse
Bbc3 (Puma)	Mm00519268_m1	Mouse
Bcl2	Mm00477631_m1	Mouse
Bcl2l1	Mm00437783_m1	Mouse
Becn1	Mm01265461_m1	Mouse
Casp12	Mm00438038_m1	Mouse
Casp3	Mm01195085_m1	Mouse
Casp6	Mm01321726_g1	Mouse
Casp7	Mm00432322_m1	Mouse
Casp8	Mm00802247_m1	Mouse

Ccl2 (Mcp1)	Mm00441242_m1	Mouse
Ccl3 (Mip1a)	Mm00441259_g1	Mouse
Col1a1	Mm00801666_g1	Mouse
Ctgf	Mm01192932_g1	Mouse
Cxcl2 (Mip2)	Mm00436450_m1	Mouse
Ddit3	Mm01135937_g1	Mouse
Fn1	Mm01256744_m1	Mouse
Gabarap	Mm00490680_m1	Mouse
Gabarapl1	Mm00457880_m1	Mouse
Gabarapl2	Mm01243684_gH	Mouse
Gadd34	Mm01205601_g1	Mouse
Gapdh	Mm99999915_g1	Mouse
Havcr1 (Kim1)	Mm00506686_m1	Mouse
Hspa5 (Bip)	Mm00517691_m1	Mouse
Igf1	Mm00439560_m1	Mouse
Il1b	Mm00434228_m1	Mouse
Il6	Mm00446190_m1	Mouse
Kcnj1 (Romk)	Mm00444727_s1	Mouse
Map1lc3b	Mm00782868_sH	Mouse
Nbr1	Mm01249798_m1	Mouse
Pdgfb	Mm00440677_m1	Mouse
Rab7a	Mm00784318_sH	Mouse
Rragc	Mm00600306_m1	Mouse
Serpine1 (Pai1)	Mm00435858_m1	Mouse
Sqstm1 (P62)	Mm00448091_m1	Mouse
Tnf	Mm00443258_m1	Mouse
Tnfrsf10b (Dr5)	Mm00457866_m1	Mouse
Tnfsf10 (Trail)	Mm01283606_m1	Mouse
Trib3	Mm00454879_m1	Mouse
Umod	Mm00447649_m1	Mouse
Vps11	Mm01168594_m1	Mouse
Vps18	Mm00552119_m1	Mouse
Vps26a	Mm00446695_m1	Mouse
Vps33a	Mm00513189_m1	Mouse
Vps35	Mm00458167_m1	Mouse
ATF4	Hs00909569_g1	Human
ATG10	Hs00919718_m1	Human
ATG12	Hs01047860_g1	Human
ATG3	Hs00223937_m1	Human
BBC3	Hs00248075_m1	Human
DDIT3 (CHOP)	Hs00358796_g1	Human

GABARAP	Hs00925899_g1	Human
GAPDH	Hs02758991_g1	Human
HAVCR1 (KIM1)	Hs00930379_g1	Human
HSPA5 (BIP)	Hs00607129_gH	Human
KCNJ1 (ROMK)	Hs00165012_m1	Human
MAP1LC3B	Hs00797944_s1	Human
NBR1	Hs00245918_m1	Human
SLC12A1 (NKCC2)	Hs00165731_m1	Human
SQSTM1	Hs01061917_g1	Human
TNF	Hs00174128_m1	Human
TNFRSF10B (DR5)	Hs00366278_m1	Human
TNFSF10 (TRAIL)	Hs00921974_m1	Human
TRIB3	Hs01082394_m1	Human
UMOD	Hs00358451_m1	Human

3. Supplemental Experimental Procedures:

Characterization and therapeutic outcome study of Umod$^{C147W/+}$ line

Initial phenotyping was performed using 4 male and 4 female mice totaling 8/group for wild type and heterozygous cohorts at 6,12, and 24 weeks-of-age. Three wild type and three heterozygous male mice were assessed at 30 weeks-of-age. Littermate controls were used to mitigate any minor genetic variations. Timed urine collection, blood draw, and body weight were collected and assessed at each time point as described previously (1). For the therapeutic outcome study using TNF inhibition, soluble TNFR:Fc (Etanercept) was injected twice weekly IP from week 10 to week 16 (10mg/kg) in cohorts of sex-matched heterozygous mutant or wild type mice. An irrelevant, isotype matched control IgG antibody specific for Hen egg lysozyme (10mg/kg) was used in the control group (2, 3). These antibodies have been shown not to stimulate immune responses in rodent experimentation (2-5). For all experiments, Blood Urea Nitrogen (BUN) (Pointe Scientific) and Creatinine (Diazyme Laboratories) in sera, as well as Creatinine and u-Albumin (Exocell) in urine were assessed using colorimetric enzyme or ELISA assays at each time point as described (1). Specific gravity of urine of 24-week-old animals was measured using Siemens Healthineers Multistix and Uristix Reagent Strips (Fisher),

according to manufacturer's protocol. Tissues were processed in PLP fixative and Formalin for histology. Tissue for RNA was preserved in RNAlater (Invitrogen), or snap-frozen in liquid nitrogen for protein analysis, as described (6).

Histology

Kidneys were resected after systemic perfusion with sterile, ice-cold PBS. Paraffin-embedded sections of kidney fixed with neutral-buffered formalin were used for periodic acid–Schiff (PAS), Masson's trichrome, and picrosirius red staining. Quantification of collagen deposition and fibrosis index were performed as described (7). Briefly, 10X images were taken across the entirety of the kidney section and positive signal intensity for picrosirius and Masson's trichrome staining were independently quantified using MATLAB software.

Immunofluorescence detection and evaluation

Mouse tissues and human cells were prepared and stained as described (8). Briefly, kidneys were fixed in PLP solution for 2 hours and washed in 18% sucrose solution overnight prior to cryopreservation and cryosectioning (7 μm). For antigen detection by fluorescence, primary antibodies against the following proteins were used for immunolabeling: Uromodulin (1:50, R&D, MAB5175, clone # 774056), Calnexin (1:200, Abcam, ab22595), Cleaved-Caspase-3 (1:400, Cell Signaling Technology, 9664, clone # 5A1E), Fibronectin (1:400, Abcam, ab6584), Laminin (1:400, Abcam, ab11575). Tissue sections were incubated with either Alexa Fluor 488 or Alexa Fluor 594 affinity purified secondary antibody (Jackson ImmunoResearch, 1:400) for 1 hour at room temperature and post-fixed with 1% paraformaldehyde/PBS. Samples were mounted in ProLong Gold reagent with DAPI (Thermo Scientific). Images were captured by confocal (Zeiss L710) as described (7).

Quantitative PCR

Total RNA was extracted from cells or whole tissue using RNeasy Plus Mini Kit (Qiagen). Purity was determined by A260 to A280 ratio. cDNA was synthesized using

oligo(dT) and random primers (iScript Reverse Transcription Supermix, Biorad). Quantitative PCR was performed using QuantStudio™ 7 Flex Real-Time PCR System (Life Technologies) using the TaqMan® Gene Expression Assays (Life Technologies). The specific primer pairs used in Q-PCR are listed in Table S1. For *Xbp1* sliced and un-spliced isoform detection, a custom Taqman primer-probe set was synthesized according to the sequences described (9). The primer sequences are as follows (nucleotide difference between *Xbp1s* and *Xbp1u* in bold): Forward 5'-CTGAGTCCGCAGCA**GGT**-3' (*Xbp1s*), 5'-CTGAGTCCGCAGCA**CTCAGA**-3'(*Xbp1u*); Reverse 5'-**TG**TCAGAGTCCATGGGAAGA-3'(*Xbp1s*), 5'TCAGAGTCCATGGGAAGA**TGTTC**-3' (*Xbp1u*); (FAM-probe): 5'-**GGCCCAGTTGTCACCTCCCC**-3' (*Xbp1s*), 5'-**CTATGTGCACCTCTGC**-3' (*Xbp1u*).

Protein isolation and western blotting

Cultured cells and snap-frozen kidney were lysed in ice-cold RIPA cell lysis buffer (Boston Bioproducts) with HALT protease and phosphatase inhibitor cocktail (Thermo Scientific), using the Omni Bead Ruptor to homogenize tissue. Samples were centrifuged for 5 minutes at 14,000 *g*, and the supernatant was taken for protein determination. Cell extracts containing 15µg protein were prepared in SDS sample buffer and subjected to SDS-PAGE. After transfer to nitrocellulose paper and blocking, immunostaining was performed in TBST buffer. The following antibodies were used to detect the specific proteins: Uromodulin (1:500, R&D, MAB5175, clone # 774056), Laminin (1:1000, Abcam, ab11575), Fibronectin (1:2000, Abcam, ab6584), Kim1 (1:1000, Abcam, ab47635), Pai1 (1:1000, Abcam, ab66705), CTGF (1:1000, Novus Biologicals, NBP2-16025), aSMA (1:1000, Abcam, ab32575, clone # E184), CHOP (1:1000, Cell Signaling Technologies, 5554S, clone # D46F1), CREB2 (1:200, Santa Cruz, sc-22800), TRIB3 (1:500, Santa Cruz, sc-34211), Caspase-12 (1:1000, Abcam, ab62484), Cleaved-Caspase-3 (1:500, Cell Signaling Technology, 9664, clone # 5A1E), p-Foxo3a (1:1000, Abcam, ab62484, clone # EPR1951(2)), Foxo3a (1:1000, Cell Signaling Technology, 12829, clone # D19A7), p-AKT (1:1000, Cell Signaling Technology, 4060, clone # D9E), AKT (1:1000, Cell Signaling Technology, 4685, clone # 11E7), p-mTOR (1:1000, Cell

Signaling Technology, 5536, clone # D9C2), p-ULK1 Ser757 (1:1000, Cell Signaling Technology, 6888), p-TFEB (1:10000, Millipore, ABE1971), SQSTM1/P62 (1:1000, Cell Signaling Technology, 12829), LC3B (1:1000, Novus Biologicals, NB100-2220) and Gapdh (1:1000, Santa Cruz, sc-20357). Bound primary antibodies were labeled with HRP-conjugated anti-rabbit or anti-mouse IgG antisera (1:3000, GE Healthcare), or anti-rat (1:3000, Thermo Scientific) or anti-goat (1:10,000, Thermo Scientific). Positive bands were detected by enhanced chemiluminescence (ECL, Pierce; SuperSignal West Dura, Thermo Scientific), and luminescence was captured by the ChemiDoc MP Imaging System (Bio-Rad). Blots were stripped with Restore buffer (Thermo Scientific) and re-probed for GAPDH. Densitometry quantification was performed in ImageJ software.

RNA sequencing and bioinformatics analysis

RNA was isolated directly from whole kidney and UMOD producing cell samples homogenized in RLT buffer and purified using RNeasy Plus Mini Kit (Qiagen). RNA quality was assessed using a Bioanalyzer (Agilent Technologies). The library preparation was done using TruSeq® Stranded mRNA Sample preparation kit (Illumina inc). The starting material (100 ng) of total RNA was mRNA enriched using the oligodT bead system. The isolated mRNA was subsequently fragmented using enzymatic fragmentation. Then first strand synthesis and second strand synthesis were performed and the double stranded cDNA was purified (AMPure XP, Beckman Coulter). The cDNA was end repaired, 3' adenylated and Illumina sequencing adaptors ligated onto the fragments ends, and the library was purified (AMPure XP). The mRNA-stranded libraries were pre-amplified with PCR and purified (AMPure XP). The libraries size distribution was validated and quality inspected on a Bioanalyzer high sensitivity DNA chip (Agilent Technologies). High quality libraries were quantified using qPCR, the concentration normalized and the samples pooled according to number of reads. The library pool(s) were re-quantified with qPCR and optimal concentration of the library pool used to generate the clusters on the surface of a flowcell before sequencing on HiSeq2500 instrument using hiSeq v.4 reagents (51 cycles). 30 million reads (50bp single-end reads) were generated and mapped onto Mus musculus reference genome GRCm38, with annotation reference Ensembl_70. Tophat (v2.0.11) and Bowtie2 (v.2.2.2) were used to

align sequence reads to the reference genome. Cufflinks (v.2.2.1)was used to convert aligned sequences into transcripts, providing map of transcriptome. Fragment bias correction was performed as described (10). Cuffdiff was used to calculate the FPKM (number of fragments per kilobase per million mapped fragments) and test for differential expression and regulation among the assembled transcripts across the submitted samples using the Cufflinks output. KEGG pathway analysis and biological process were performed using STRING (v10.0 String Consortium 2016) on the top 40 differentially expressed genes with FDR<0.05 and Log_2FC >1. Biological process gene ontology enrichment analysis was also performed using open source software from the Gene Ontology Consortium, as a second means of verification. To analyze for transcription factor activity, Whole Genome RVista was used (genome.lbl.org). Detailed RNAseq information including access to raw data, meeting Minimum Information About a Microarray Experiment (MIAME) requirements, has been deposited in the NCBI's Gene Expression Omnibus (GSE102566).

Cell purification, culture, and assays

Purification of cells from kidney

Mouse UMOD producing epithelial cell purification was performed by preparing single cell digest from normal and diseased mouse kidney, as described (7, 11), with modifications. Briefly, kidneys were decapsulated, minced, and then incubated in a shaking water bath (180 rpm) at 37°C for 50 min with Liberase DL (0.5mg/mL; Roche) and DNase (100U/mL; Roche) in serum-free DMEM/F12. After incubation, enzymatic digestion was halted by addition of 1 volume (2mLs) of DMEM/F12 with 10% serum. The tissue digest was mixed thoroughly and filtered (40μM).

UMOD producing cells were separated from the single cell suspension using the Dynabead magnetic bead conjugation system, whereby biotinylated, mouse anti-UMOD monoclonal antibody (R&D: BAF5175) was incubated with Dynabeads Biotin Binder (Thermo Fisher). For each kidney isolate, 100uL beads were conjugated with 6μg anti-UMOD antibody at 4°C for 45min. Beads were then washed twice with MACS buffer, and incubated with the single cell suspension in a final volume of 1mL at 4°C for 45min. Beads and UMOD cells were then trapped against a magnet, and residual UMOD-

negative cells were washed away. UMOD cell positive fractions were divided and harvested immediately for RNA in RLT buffer (Qiagen) with 2-mercaptoethanol (Sigma), or for protein analysis in RIPA Buffer (Boston Bioproducts) with 2X Halt Protease and Phosphatase buffer (Thermo Scientific). Murine LTL+ proximal tubule cells were isolated from the UMOD negative fraction, as a negative control, in the same manner described above with use of Biotinylated LTL (Vector Laboratories, 2ug LTL/5uL Dynabead suspension). UMOD producing cells were isolated from discarded human kidney from nephrectomies performed at Tufts New England Medical Center (Boston, MA). The procedure is identical to that for mouse listed above, with the exception of the antibody for isolation being biotinylated, human-UMOD monoclonal antibody (R&D: BAF5144). LTL+ proximal tubule cells and then EPCAM+ cells were sequentially isolated from the remaining UMOD negative fraction as controls. LTL+ cells were isolated using Biotin Binder Dynabeads and Biotinylated LTL (Vector Laboratories, B-1325) (2ug LTL/5uL Dynabead suspension), as described above. EPCAM+ cells were isolated using CD326 (EpCAM) MicroBeads (Miltenyi Biotec) and MACS LS columns (Miltenyi Biotec), as previously described (8). A fraction of each of the human UMOD producing, LTL+, and EPCAM+ cell isolates were immediately harvested for RNA in RLT buffer (Qiagen), and the remainder were cultured and maintained as independent cultures in complete Renal Epithelial Growth Medium (REGM, Lonza).

Transgenic expression and gene silencing in vitro

Stable expression of mutant p.Cys147Trp and wild type UMOD, driven under the CMV promoter, was established in human UMOD positive cells using lentiviral vectors purchased from GeneCopoeia. Positive selection of transduced cells was achieved with puromycin treatment at 1μg/mL. The human, transgenic UMOD cell populations were immortalized with transduction with a CMV-temperature sensitive SV40 TAg viral vector. Human cell lines of each transgenic primary culture were established and maintained at 33°C, and cultured for 48hrs at 37°C to equilibrate prior to experimentation.

Autophagy-flux detection assay

Uromodulin positive human tubule cells expressing UMOD p.Cys147Trp mutation were plated at 35,000 cells per well in a black, clear bottom 96-well plate, and transduced with Premo Autophagy Tandem Sensor LC3B-GFP-RFP BacMam 2.0 virus (Thermo Scientific) according to the vendor's protocol for 24hrs. Cells were then treated with 0.1% DMSO (Sigma), 12.5-50nM Rapamycin (Sigma), or 5-20uM Torkinib (Selleckchem) in Opti-Mem (Thermo Scientific). Fluorescent (Red/Green) and phase contrast images (4 images per well) were captured using a commercially available imaging system (IncuCyte ZOOM, Essen BioScience, Ann Arbor, MI, USA) at 6 and 12 hrs post treatment, and quantification for percent loss of LC3B-GFP-RFP overlap signal was performed.

Apoptosis detection assay and ER stress induction

Uromodulin primary human p.Cys147Trp mutant or wild type cells were plated at 50,000 cells per well in a black, clear bottom 96-well plate, and cultured for 16hrs in growth media. Cells were then transfected with non-targeting control, or TRIB3 siRNA as described above. After 24hrs, cells were pulsed for 4 hours with 10ug/mL Brefeldin A (Cell Signaling Technology) to simulate an ER-stress insult. Cells were then allowed to recover in growth media for 20 hours. After recovery, cells were stimulated with 50ng/mL TNFα (Life Technologies) or 50ng/mL TRAIL (Gibco) in Opti-Mem. CellEvent Caspase-3/7 Green ReadyProbes Reagent (Thermo Scientific) was included in the vehicle and cytokine treatments as per supplier's instructions (2 drops/mL). Upon cytokine treatment, wells were imaged at 4 images per well over 24 hours with the InCucyte ZOOM imaging system. The number of positive, cleaved caspase-3,7 puncta per image was quantified over 24 hours.

4. Supplemental References:

1. Gomez IG, MacKenna DA, Johnson BG, Kaimal V, Roach AM, Ren S, Nakagawa N, Xin C, Newitt R, Pandya S, et al. Anti-microRNA-21 oligonucleotides prevent Alport nephropathy progression by stimulating metabolic pathways. *The Journal of clinical investigation.* 2015;125(1):141-56.

2. Xia Y, Campbell SR, Broder A, Herlitz L, Abadi M, Wu P, Michaelson JS, Burkly LC, and Putterman C. Inhibition of the TWEAK/Fn14 pathway attenuates renal disease in nephrotoxic serum nephritis. *Clinical immunology.* 2012;145(2):108-21.
3. Fernandez-Laso V, Sastre C, Mendez-Barbero N, Egido J, Martin-Ventura JL, Gomez-Guerrero C, and Blanco-Colio LM. TWEAK blockade decreases atherosclerotic lesion size and progression through suppression of STAT1 signaling in diabetic mice. *Scientific reports.* 2017;7(46679.
4. Abdul-Hamid M, Ahmed RR, Moustafa N, and Nady R. The antifibrogenic effect of etanercept on development of liver cirrhosis induced by thioacetamide in rats. *Ultrastructural pathology.* 2017;41(1):23-35.
5. Nakagawa H, Umemura A, Taniguchi K, Font-Burgada J, Dhar D, Ogata H, Zhong Z, Valasek MA, Seki E, Hidalgo J, et al. ER stress cooperates with hypernutrition to trigger TNF-dependent spontaneous HCC development. *Cancer cell.* 2014;26(3):331-43.
6. Ren S, Johnson BG, Kida Y, Ip C, Davidson KC, Lin SL, Kobayashi A, Lang RA, Hadjantonakis AK, Moon RT, et al. LRP-6 is a coreceptor for multiple fibrogenic signaling pathways in pericytes and myofibroblasts that are inhibited by DKK-1. *Proceedings of the National Academy of Sciences of the United States of America.* 2013;110(4):1440-5.
7. Ren S, Johnson BG, Kida Y, Ip C, Davidson KC, Lin SL, Kobayashi A, Lang RA, Hadjantonakis AK, Moon RT, et al. LRP-6 is a coreceptor for multiple fibrogenic signaling pathways in pericytes and myofibroblasts that are inhibited by DKK-1. *Proceedings of the National Academy of Sciences of the United States of America.* 2013;110(4):1440-5.
8. Gomez IG, MacKenna DA, Johnson BG, Kaimal V, Roach AM, Ren S, Nakagawa N, Xin C, Newitt R, Pandya S, et al. Anti-microRNA-21 oligonucleotides prevent Alport nephropathy progression by stimulating metabolic pathways. *The Journal of clinical investigation.* 2015;125(1):141-56.
9. Hayashi A, Kasahara T, Iwamoto K, Ishiwata M, Kametani M, Kakiuchi C, Furuichi T, and Kato T. The role of brain-derived neurotrophic factor (BDNF)-induced XBP1 splicing during brain development. *The Journal of biological chemistry.* 2007;282(47):34525-34.
10. Hansen KD, Brenner SE, and Dudoit S. Biases in Illumina transcriptome sequencing caused by random hexamer priming. *Nucleic acids research.* 2010;38(12):e131.
11. Schrimpf C, Xin C, Campanholle G, Gill SE, Stallcup W, Lin SL, Davis GE, Gharib SA, Humphreys BD, and Duffield JS. Pericyte TIMP3 and ADAMTS1 modulate vascular stability after kidney injury. *Journal of the American Society of Nephrology : JASN.* 2012;23(5):868-83.